09

Optical properties of a thin nickel film exposed to high-intensity terahertz pulses

© O.V. Chefonov[1], S.A. Evlashin[2], M.A. Ovchinnikova[1], I.V. Il'ina[1], A.V. Ovchinnikov[1]

[1] Joint Institute for High Temperatures, Russian Academy of Sciences, Moscow, Russia
[2] Skolkovo Institute of Science and Technology, Moscow, Russia
E-mail: ovtch2006@yandex.ru

Received October 16, 2025
Revised November 18, 2025
Accepted December 10, 2025

The paper presents the results of experimental studies of the complex refractive index of a thin nickel film exposed to subpicosecond terahertz pulses with the electric field strength of 0.5−10 MV/cm. A 20 nm thick nickel film deposited on a 160 μm thick glass substrate was used in the experiments. The studies were conducted in the spectral range of 0.25−2.25 THz.

Keywords: terahertz radiation, thin nickel film, complex refractive index, optical constants.

DOI: 10.61011/TPL.2026.04.63204.20531

In recent years, research in the field of generating subpicosecond pulses of terahertz (THz) radiation has led to development of a variety of sources with a wide range of electric field strengths and different pulse repetition rates [1,2]. Such sources may be applied in various fields of science and technology, for instance, in materials spectroscopy, medicine, wireless communications, etc. [3]. Controlling the parameters and recording signals of THz radiation requires the use of passive optical elements (including waveguides, filters [4] and mirrors), as well as of sensitive detectors, such as microbolometer receivers [5]. In such devices, thin (nanometer-thick) metal films are widely used.

Optical properties of metal films in the THz-spectral range have been studied at low electric fields ($\ll$ 100 kV/cm) [6,7]; experimental data for high fields are still unavailable. In [8] it was theoretically shown that the impact on aluminum nanofilms from THz-pulses with the field of up to 90 MV/cm leads to significant variations in the transmission and reflection coefficients.

This paper presents the results of experimental studies of the complex refractive index of the Ni film 20 nm thick in the spectral range of 0.25−2.25THz under the impact of THz pulses with electric fields of up to 10 MV/cm. Optical properties were studied by THz time-domain spectroscopy [9]. This method involves measuring time profiles of THz pulses incident on and transmitted through the sample under study, which was followed by Fourier transform calculation of the spectra and calculation of the medium's optical characteristics.

Fig. 1 presents the schematic diagram of the experiment. Subpicosecond THz pulses were generated by optical rectification of femtosecond pulses of a chromium-forsterite laser system with the radiation wavelength of 1240 nm, pulse energy of up to 30 mJ and pulse repetition rate of 10 Hz in the nonlinear organic crystal OH1 [10]. THz radiation was focused onto the sample via a system of off-axis parabolic mirrors. The beam radius measured by the THz-camera in the focal plane was $156 \pm 9\,\mu$m at the level of $1/e^2$ from the maximum intensity. Temporal profile of the THz pulse electric field was measured by electro-optical detection [9] in a GaP crystal 200 μm thick using a probing pulse 100 fs long with the wavelength of 1240 nm. To maintain the linear operating mode of the measuring circuit, the THz-pulse field incident on the GaP crystal was attenuated by a pair of film polarizers. The THz pulse energy was measured by a calibrated Golay cell (optoacoustic detector GC-1D, Tydex) in the beam waist where the experimental sample was installed. The THz-pulse energy was controlled by varying with a polarization attenuator the energy of a laser pulse pumping the nonlinear organic crystal.

In the experiments, peak THz-pulse electric field E_0 was estimated through peak intensity $E_0 = (2Z_0 I_0)^{1/2}$ based on the experimentally measured THz-pulse parameters (energy, beam radius, and duration) under the assumption that the spatial-temporal intensity profile has Gaussian shape $I_0 = 2P_0/\pi w^2$, where $Z_0 = 377\,\Omega$ is the vacuum wave impedance, $P_0 \approx 0.94\,W_{\mathrm{THz}}/\tau_{\mathrm{FWHM}}$ is the peak pulse power, w is the beam radius at the level of $1/e^2$, W_{THz} is the THz-pulse energy, $\tau_{\mathrm{FWHM}} = 450$ fs is the pulse duration measured as full width at half maximum of the THz pulse intensity profile $|E_t|^2$, and also in the electro-optical detection circuit [11,12]. The maximum experimental electric field magnitude was $\sim$ 10 MV/cm.

The measurements were performed in a closed box into which dried air with relative humidity not higher than 2 % was supplied. This allowed the water vapor impact on the spectral measurements to be reduced.

The sample was a 20 nm thick nickel film deposited on a polished glass substrate 160 μm thick by magnetron sputtering at the rate of 1 nm/s in argon (99.999 % purity) at the pressure of 50 MPa.

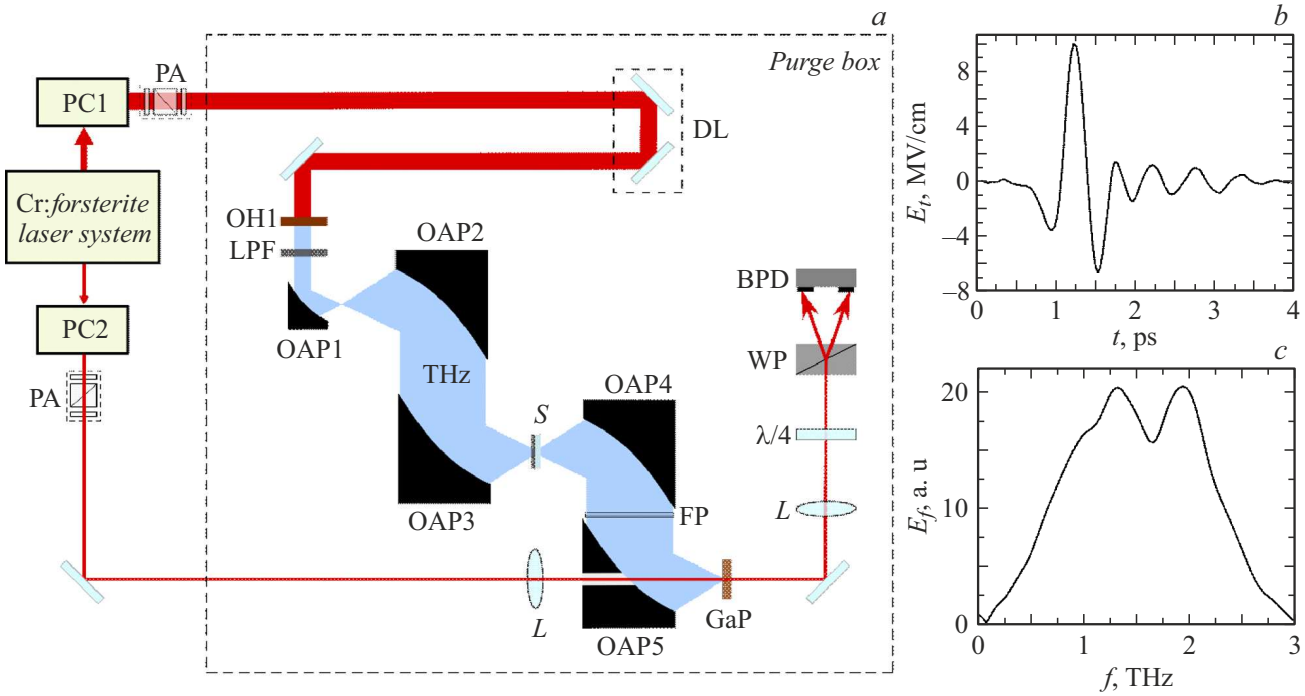

Figure 1. *a* — experiment schematic diagram. PC1 and PC2 — pump and probe pulse time compressors, respectively, PA — polarization attenuator, DL — time delay, LPF — terahertz low-pass filter, OAP1–5 — off-axis parabolic mirrors, THz — THz radiation, *S* — sample, *L* — lens, $\lambda/4$ — quarter-wave plate, WP — Wollaston prism, BPD — balanced photodetector, FP — film polarizers; *b* — temporal shape of the THz-pulse electric field; *c* — THz radiation spectrum.

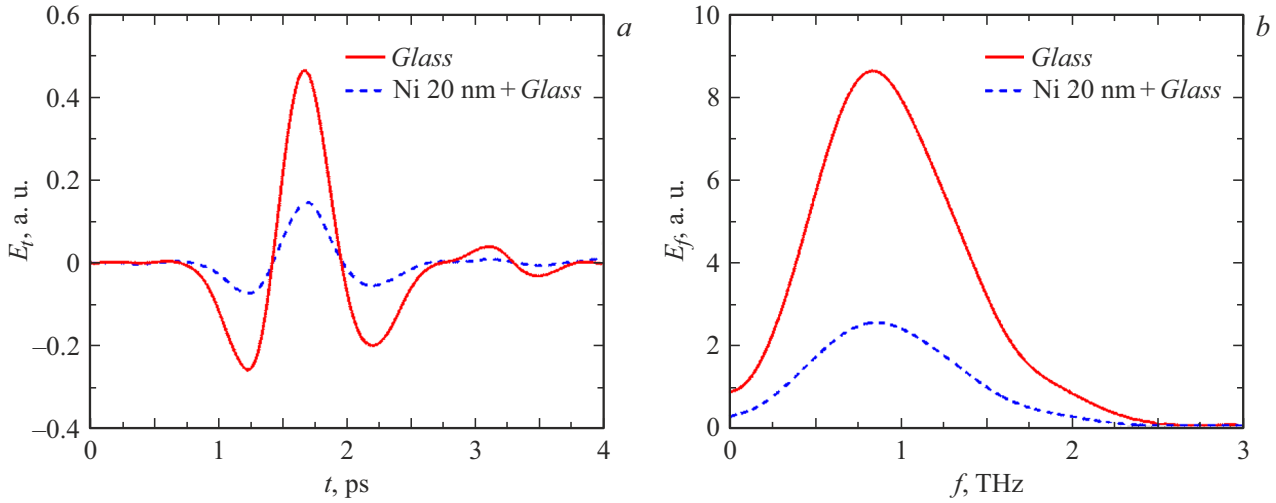

Figure 2. Temporal shapes of THz pulses of the substrate and sample (*a*) and respective Fourier spectra (*b*) for the incident field of 500 kV/cm.

At the first stage of determining the nickel film's complex refractive index, there were measured temporal shapes of THz pulses that have passed through glass substrates without and with the film. After that, the THz spectrum of the metal film's complex amplitude transmittance $\tilde{t}_{meas}(\omega)$ involving the film amplitude and phase was calculated as a ratio between the substrate-with-film and substrate spectra. Fig. 2 demonstrates temporal shapes of THz pulses passed through the substrate and sample, as well as respective amplitude spectra measured for the field of 500 kV/cm.

The thin nickel film is characterized by complex refractive index $\tilde{n}_{sam}$ and thickness d; respective parameters of the substrate are $\tilde{n}_{sub}$ and L. In addition, the sample is placed in ambient air with complex refractive index $\tilde{n}_{air} = 1$. The nickel film's complex amplitude transmittance at cyclic

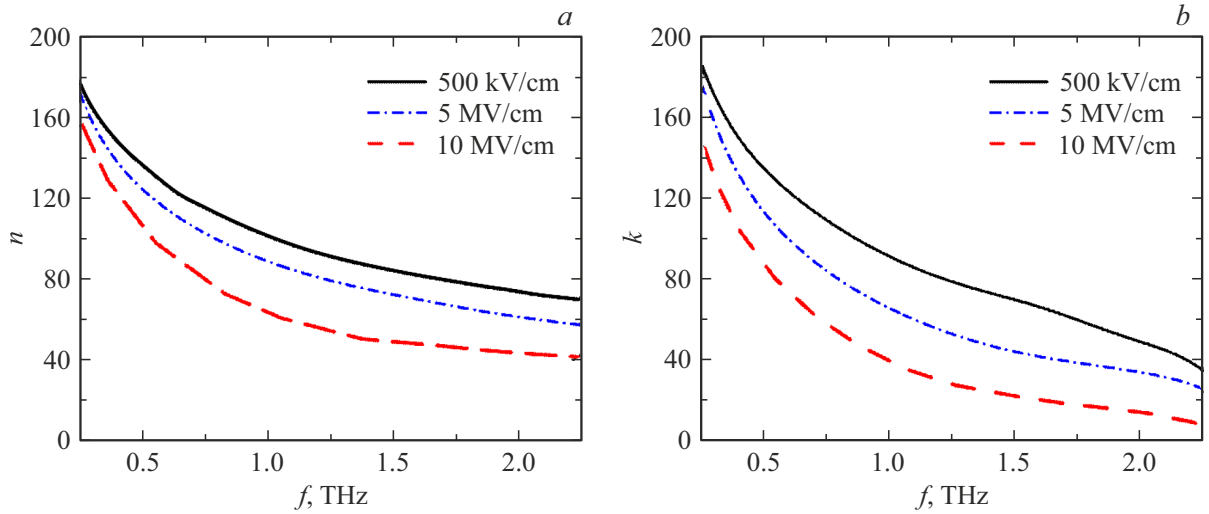

Figure 3. Spectral dependences of the real (a) and imaginary (b) parts of the complex refractive index of the 20 nm thick nickel film exposed to THz pulses with different electric field magnitudes.

frequency ω is defined as follows [13]:

$$\tilde{t}_{sam}(\omega) = \frac{2\tilde{n}_{sam}(\tilde{n}_{air}+\tilde{n}_{sub})}{(\tilde{n}_{sam}+\tilde{n}_{air})(\tilde{n}_{sam}+\tilde{n}_{sub})} \times \exp\left(-i\left(\tilde{n}_{sam}-\tilde{n}_{air}\right)\frac{\omega d}{c}\right)FP(\omega), \qquad (1)$$

where c is the speed of light in vacuum. Factor

$$FP(\omega) = \left[1-\left(\frac{\tilde{n}_{sam}-\tilde{n}_{air}}{\tilde{n}_{sam}+\tilde{n}_{air}}\right)\left(\frac{\tilde{n}_{sam}-\tilde{n}_{sub}}{\tilde{n}_{sam}+\tilde{n}_{sub}}\right) \times \exp\left(-i2\tilde{n}_{sam}\frac{\omega d}{c}\right)\right]^{-1}$$

in (1) accounts for the THz radiation multipath interference in the thin film.

The procedure for deriving the thin film's complex refractive index $\tilde{n}_{sam} = n_{sam} - ik_{sam}$ as a function of frequency ω consisted in numerically solving equation (1) whose left-hand side was the measured nickel film's complex amplitude transmittance $\tilde{t}_{meas}(\omega) = |\tilde{t}_{meas}|\exp(i\varphi) = \tilde{t}_{sam}(\omega)$, where φ is the complex transmittance phase [7]. Thus, a set of two equations was solved for n_{sam} and k_{sam} for each pair of amplitude $|\tilde{t}_{meas}|$ and phase φ of the film's complex amplitude transmittance. Complex refractive index $\tilde{n}_{sub} = n_{sub} - ik_{sub}$ of the glass substrate was measured separately. In the range of 0.25–2.25 THz, the refractive index real part varied slightly and amounted to $n_{sub} \sim 2.5$. Imaginary part k_{sub} increased with increasing frequency and did not exceed unity. The substrate's complex refractive index did not change at all the electric fields at which the nickel film's complex refractive index was measured. Experimental data on the glass substrate's complex refractive index were used to solve equation (1) in determining the film optical characteristics.

The measurements were performed at three magnitudes of the THz-pulse electric fields: 500 kV/cm, 5 MV/cm and 10 MV/cm. Fig. 3 presents the calculated frequency dependences of the complex refractive index real and imaginary parts for the nickel film 20 nm thick. The obtained dependences show that the real and imaginary parts of the complex refractive index decrease with increasing applied electric field of the THz-pulse.

Study [14] has shown that when the nickel film 25 nm thick is exposed to THz pulses with electric field of $\sim$ 11 MV/cm, the electron subsystem gets strongly excited, and a two-temperature state arises, in which the electron temperature significantly exceeds the lattice one. In contrast to the results presented in [14], our experiments exhibited no melting of the nickel film, despite close magnitudes of the THz-pulse electric field. This was because energy density of pulses used in our study was $\sim$ 1.5 times lower than in [14]. Note that the field magnitudes were close because the THz-pulse from the OH1 crystal was shorter than that in the case of the DSTMS crystal used in [14].

Thus, we can conclude that the estimates of optical constants of the nickel film 20 nm thick obtained from experimental measurements under the impact of THz pulses with electric field of 10 MV/cm match those of the film in the two-temperature state. The experimentally observed changes in the optical constants depending on the THz pulse field may be associated with an increase in the electron collision frequency [8]. Note in conclusion that the experimental approach implemented in this work can help in studying optical properties of thin metal films in a nonequilibrium state under the impact of high-electric-field THz-pulses.

Acknowledgements

The experiments were performed on a unique terawatt chromium-forsterite laser system (UNU „LTFC“) at the JIHT RAS Common Use Center „Laser Femtosecond Complex“.

Funding

The study was supported by the Russian Science Foundation, project No 24-19-00311 (https://rscf.ru/project/24-19-00311/).

Conflict of interests

The authors declare that they have no conflict of interests.

References

[1] S. Mansourzadeh, T. Vogel, A. Omar, T.O. Buchmann, E.J.R. Kelleher, P.U. Jepsen, C.J. Saraceno, Opt. Mater. Express, **13** (11), 3287 (2023). DOI: 10.1364/ome.502209
[2] S. Makhlouf, O. Cojocari, M. Hofmann, T. Nagatsuma, S. Preu, N. Weimann, H.-W. Hübers, A. Stöhr, IEEE J. Microwaves, **3** (3), 894 (2023). DOI: 10.1109/JMW.2023.3282875
[3] A. Leitenstorfer, A.S. Moskalenko, T. Kampfrath, J. Kono, E. Castro-Camus, K. Peng, N. Qureshi, D. Turchinovich, K. Tanaka, A.G. Markelz, M. Havenith, C. Hough, H.J. Joyce, W.J. Padilla, B. Zhou, K.-Y. Kim, X.-C. Zhang, P.U. Jepsen, S. Dhillon, M. Vitiello, E. Linfield, A.G. Davies, M.C. Hoffmann, R. Lewis, M. Tonouchi, P. Klarskov, T.S. Seifert, Y.A. Gerasimenko, D. Mihailovic, R. Huber, J.L. Boland, O. Mitrofanov, P. Dean, B.N. Ellison, P.G. Huggard, S.P. Rea, C. Walker, D.T. Leisawitz, J.R. Gao, C. Li, Q. Chen, G. Valušis, V.P. Wallace, E. Pickwell-MacPherson, X. Shang, J. Hesler, N. Ridler, C.C. Renaud, I. Kallfass, T. Nagatsuma, J.A. Zeitler, D. Arnone, M.B. Johnston, J. Cunningham, J. Phys. D, **56** (22), 223001 (2023). DOI: 10.1088/1361-6463/acbe4c
[4] M. Han, D. Smith, S.H. Ng, Z. Vilagosh, V. Anand, T. Katkus, I. Reklaitis, H. Mu, M. Ryu, J. Morikawa, J. Vongsvivut, D. Appadoo, S. Juodkazis, Micromachines, **13** (8), 1170 (2022). DOI: 10.3390/mi13081170
[5] M.A. Demýanenko, I.V. Marchishin, V.V. Startsev, OSA Continuum, **2** (6), 2085 (2019). DOI: 10.1364/osac.2.002085
[6] F.-Y. Ma, J.-P. Su, Q.-X. Gong, J. Yang, Y.-L. Du, M.-T. Guo, B. Yuan, Chin. Phys. Lett., **28** (9), 097803 (2011). DOI: 10.1088/0256-307X/28/9/097803
[7] D.-X. Zhou, E.P.J. Parrott, D.J. Paul, J.A. Zeitler, J. Appl. Phys., **104** (5), 053110 (2008). DOI: 10.1063/1.2970161
[8] S.G. Bezhanov, S.A. Uryupin, Opt. Lett., **43** (13), 3069 (2018). DOI: 10.1364/ol.43.003069
[9] M. Koch, D.M. Mittleman, J. Ornik, E. Castro-Camus, Nat. Rev. Meth. Primers, **3** (1), 48 (2023). DOI: 10.1038/s43586-023-00232-z
[10] A.V. Ovchinnikov, O.V. Chefonov, M.B. Agranat, M. Shalaby, D.S. Sitnikov, Opt. Lett., **47** (21), 5505 (2022). DOI: 10.1364/ol.475960
[11] X. Ropagnol, C. Garcia-Rosas, H. Uchida, F. Blanchard, T. Ozaki, J. Phys. Photon., **7** (4), 045002 (2025). DOI: 10.1088/2515-7647/adf168
[12] A.V. Ovchinnikov, I.V. Il'ina, M.A. Ovchinnikov, O.V. Chefonov, Opt. Lett., **49** (21), 6021 (2024). DOI: 10.1364/ol.534216
[13] L. Duvillaret, F. Garet, J.-L. Coutaz, IEEE J. Sel. Top. Quantum Electron., **2** (3), 739 (1996). DOI: 10.1109/2944.571775
[14] S.I. Ashitkov, P.S. Komarov, A.V. Ovchinnikov, S.A. Romashevskiy, E.V. Struleva, O.V. Chefonov, M.B. Agranat, JETP Lett., **120** (8), 580 (2024). DOI: 10.1134/S002136402460349X.

Translated by EgoTranslating